NON-NEUTRAL PLASMA TRAPS FOR ACCELERATOR-FREE EXPERIMENTS ON SPACE-CHARGE-DOMINATED BEAM DYNAMICS

Hiromi Okamoto, Hiroyuki Higaki, Kiyokazu Ito
AdSM, Hiroshima University, 1-3-1 Kagamiyama, Higashi-Hiroshima 739-8530, Japan

Abstract

The beam physics group of Hiroshima University has developed compact plasma trap systems to explore diverse fundamental aspects of space-charge-dominated beam dynamics. At present, two Paul ion traps are in operation, one more under construction, and a Penning-Malmberg type trap is also working. These very compact, accelerator-free experiments are based on the isomorphism between a non-neutral plasma in a trap and a charged-particle beam traveling in a periodic focusing channel. Systematic studies of coherent betatron resonances, ultralow-emittance beam stability, and halo formation are in progress employing both types of traps. Latest experimental results and possible future plans are addressed in this paper.

INTRODUCTION

The progress of various accelerator technologies has made it feasible to realize high-power or high-density beams of charged particles, which inevitably increases the importance of understanding "space-charge effects (SCE)" [1]. It is, however, generally quite troublesome to perform systematic investigations of SCE. Experimentally, we encounter many limitations originating from poor controllability of machine parameters. For instance, betatron tunes cannot be varied over a wide range and, needless to say, the lattice structure is fixed once the machine is constructed. High precision and resolution measurements are difficult because the beam is moving at relativistic speed in the laboratory frame. Furthermore, too much beam losses, which might damage the machine, are unacceptable in practice. This means that we cannot actually carry out high-power beam experiments as long as we rely on real accelerators.

Theoretically, complete information of collective beam behavior is obtained from the phase-space distribution function f that approximately satisfies the Vlasov equation

$$\frac{\partial f}{\partial s} + [H, f] = 0, \tag{1}$$

where the independent variable s is the path length along the design beam orbit, and [,] stands for the Poisson bracket. The Hamiltonian H includes the scalar potential ϕ that is the source of SCE and obeys the Poisson equation

$$\Delta\phi = -\frac{e}{\varepsilon_0}\rho, \tag{2}$$

where e is the charge state of the particles, and the number density ρ can be calculated by integrating the distribution function f over the momentum space. The self-consistent treatment of these equations is clearly very difficult and, therefore, we are forced to introduce mathematical models. Although high-performance computers enable us to provide better predictions of the beam behavior, we still need proper models (e.g. macro-particles, symmetry assumptions, etc.) to save CPU time.

An alternative experimental approach, totally free from the above-mentioned difficulties in accelerator-based studies, was first proposed by Okamoto and Tanaka over ten years ago [2,3]. The new method exploits the simple fact that a non-neutral plasma in a tabletop trap system can be physically almost equivalent to a relativistic beam observed in the center-of-mass frame. We have developed, in Hiroshima, several trap systems dedicated to beam physics purposes, which we call "S-POD (Simulator for Particle Orbit Dynamics)". The first and second S-PODs are based on radio-frequency (RF) confinement [4], and there is another system using magnetic confinement. The third RF trap is now under construction. Each trap system has been optimized to explore different beam dynamics issues including resonance instabilities, an ultralow-emittance ion source, and halo formation [5,6]. Except for Hiroshima, only one team in Princeton has been using a non-neutral plasma trap for beam physics [7-9]. The core of the Princeton system, referred to as "PTSX (Paul Trap Simulator Experiment)", is a cylindrical RF trap of 280 cm long.

NON-NEUTRAL PLASMA TRAPS

Similarly to the case of accelerator beams, the distribution function of charged particles confined in a trap is governed by the Vlasov equation (1) and the self-field scalar potential satisfies the Poisson equation (2). Therefore, the only question is how the Hamiltonians of the two dynamical systems correspond to each other. For the sake of simplicity, let us consider a coasting beam traveling in a linear transport channel. The Hamiltonian of the transverse beam motion can be expressed as

$$H = \frac{p_x^2 + p_y^2}{2} + \frac{1}{2}K(s)(x^2 - y^2) + I\phi, \tag{3}$$

where I is a constant, and $K(s)$ depends on the arrangement of focusing quadrupole magnets along the beam orbit. There are, at least, two types of non-neutral plasma traps that can emulate the many-body system defined by eq. (3) [2].

Radio-Frequency Trap (*Linear Paul Trap*)

The linear focusing potential as in eq. (3) can readily be generated by an RF quadrupole in the time domain (instead of magnets in the s-domain). The basic structure of an RF quadrupole trap, often called a "linear Paul trap

(LPT)" [4], is illustrated in Fig. 1. The transverse Hamiltonian of the LPT takes the form

$$H_{\mathrm{LPT}} = \frac{p_x^2 + p_y^2}{2} + \frac{1}{2} K_{\mathrm{RF}}(t)(x^2 - y^2) + I_1 \phi, \qquad (4)$$

where I_1 is a constant, and $K_{\mathrm{RF}}(t)$ is proportional to the waveform of the RF voltage applied to the quadrupole rods. The correspondence of H_{LPT} to the beam Hamiltonian H is evident. It is thus possible for the LPT to reproduce the beam system travelling in a periodic focusing channel.

The LPT is most simply a combination of four rods producing the transverse confinement field and two end plates for longitudinal confinement. In many cases including ours, the quadrupole rods are divided into several pieces, so that we can form one or more axial potential well(s) by independently adding DC voltages to the rods. In that case, the end plates as in Fig. 1 become unnecessary.

A typical LPT designed by the Hiroshima group is shown in Fig. 2. This LPT is composed of five separate quadrupoles and has no end plates. The axial size is only less than 20 cm. Such a simple, compact devise costs very little unlike any particle accelerators. We actually have several LPTs of different designs optimized for diverse experimental purposes.

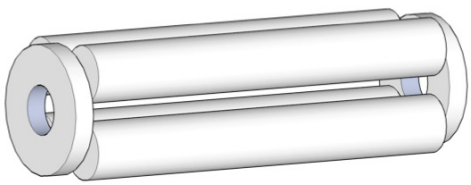

Figure 1: Fundamental structure of a linear Paul trap.

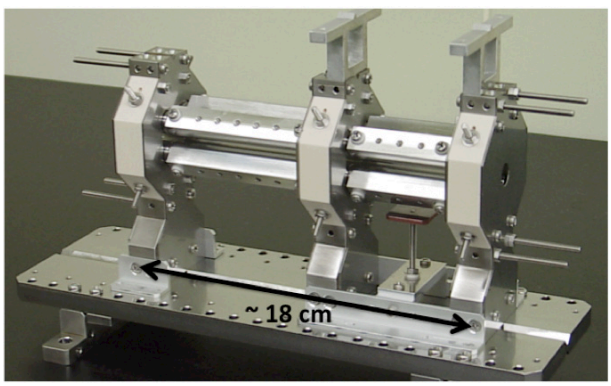

Figure 2: A multi-sectioned LPT employed for beam dynamics experiments at Hiroshima University

Magnetic Trap (Penning-Malmberg Trap)

Since the Vlasov-Poisson equations are too complex to treat analytically for general s-dependent focusing channels, we have very often made use of the smooth approximation to simplify the Hamiltonian. The beam Hamiltonian H after smoothing a linear alternating gradient (AG) lattice can be written as

$$\bar{H} = \frac{p_x^2 + p_y^2}{2} + \frac{1}{2}\kappa^2(x^2 + y^2) + I\phi, \qquad (5)$$

where κ corresponds to the phase advance (tune) per single lattice period. It is straightforward to prove that the transverse Hamiltonian for charged particles confined by a uniform magnetic field along the z-direction has the same form as eq. (5) if we observe the particle motion in a rotating frame [2].

Figure 3 is a rough sketch of our magnetic trap in which we have usually confined electrons. Since the axial magnetic field is provided by many separate solenoid coils, we can generate not only uniform but also non-uniform mirror fields. For axial confinement, 45 ring-shaped electrodes to which we can independently apply DC voltages are aligned inside the cylindrical vacuum chamber. It is possible to form different types of potential wells that enable us to study the dynamic behaviors of pure electron plasmas with various aspect ratios. In the following, we call the apparatus "multi-ring electrode trap (MRET)".

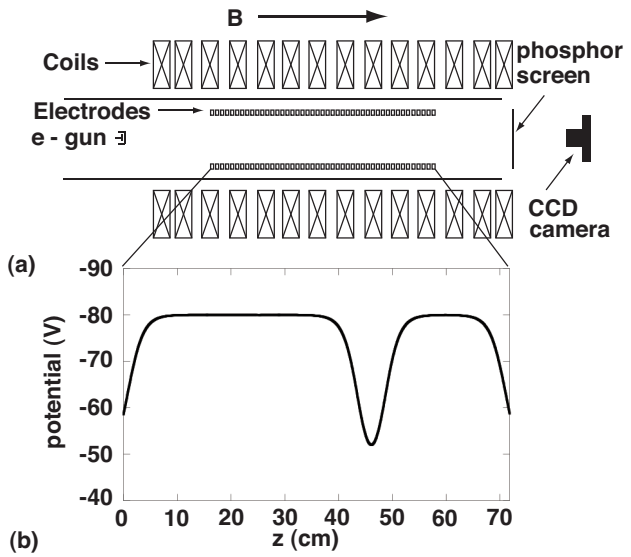

Figure 3: Multi-ring electrode trap (MRET) at Hiroshima University and its typical longitudinal electric potential for particle confinement. The transverse confinement is achieved by the axial magnetic field **B**.

S-POD

As explained in previous sections, either LPT or MRET can provide many-body systems that are approximately equivalent to charged-particle beams in linear transport channels. Taking this isomorphism into account, we have designed and constructed several S-POD systems. A picture of one of the S-PODs developed in Hiroshima is exhibited in Fig. 4. The main components of this compact experimental tool include a multi-sectioned LPT (similar but not identical to the one in Fig. 2), a vacuum system, many DC and AC power sources, a personal computer, and Doppler laser cooling system. Three different diagnostic devices are currently available, that is, a Faraday cup (FC), a micro-channel plate (MCP), and a CCD camera for laser-induced fluorescence (LIF) measurements. The power sources are controlled with the

computer and can very easily generate a wide range of periodic pulse voltages emulating various AG lattice structures.

S-POD experiments are completely automated; in typical resonance experiments discussed in the next section, for example, all we must do is to input the initial and final RF amplitudes (corresponding to the range of the bare betatron tune we survey), the number of data points (in other words, the step size of tune variation), ionization time for plasma generation, plasma storage period, and some more. Since the computer automatically repeats the necessary experimental procedures, we do not have to stay beside the S-POD to retune parameters. Typically, we switch on an electron gun for around one second to produce lots of ions, and then, store the plasma for 1 – 10 milliseconds. Since the primary RF frequency for ion focusing is set at near 1 MHz in the present system, the 10-msec plasma storage corresponds to a beam transport through 10,000 FODO cells. After this very short storage, the DC bias voltages on the end electrodes are quickly shut down to launch the plasma toward either the FC or MCP.

We have usually been using Ar^+ ions for resonance experiments so far, while it is possible to accumulate other ion species if necessary. An atomic oven is installed in the vacuum chamber, so that we can make Ca^+ plasmas coolable with the semi-conductor laser system. As the Doppler limit of laser cooling is close to the absolute zero, the tune depression of the plasma can, in principle, be controlled over the full range (from 1 to 0). At the space-charge limit, the plasma comes to a Coulomb crystalline state that is another interesting topic to pursue [6]. The use of Ca^+ plasmas is advantageous from a diagnostic point of view as well because the LIF signals can be used for very high precision measurements.

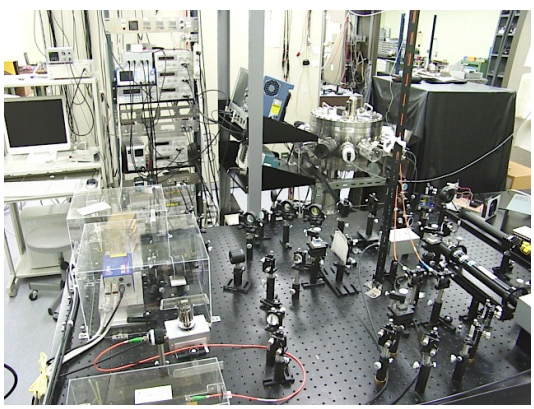

Figure 4: Overall view of a S-POD system (based on a LPT) in Hiroshima.

RESONANCE EXPERIMENTS

Coherent Resonance Instability

One of the most important beam dynamics subjects that we can study systematically with the S-PODs is the resonance instability driven by the periodicity of external focusing forces [10-12]. The collective motion of a beam (or a plasma) can be described by the superposition of various coherent modes whose oscillation tunes Ω_m (m = positive integer: mode number) depend on the particle density in phase space. The tune of one-dimensional coherent mode of m-th order can approximately be written as $\Omega_m = m(\nu_0 - C_m\Delta\nu)$ where ν_0 represents the bare tune of the single-particle motion, $\Delta\nu$ is the space-charge-induced tune shift, and C_m is the mode-dependent constant smaller than unity. When Ω_m of a particular mode is near a half integer, that mode becomes unstable [12]. The resonance condition for a circular machine with superperiodicity N_{sp} is thus given by

$$\nu_0 - C_m\Delta\nu \approx N_{sp}\cdot\frac{n}{2m}, \qquad (6)$$

where n is an integer [12]. Note that the factor 1/2 on the right hand side is missing in the famous Sacherer's resonance condition [10].

An example of experimental data obtained with a S-POD is plotted in Fig. 5. In this experiment, $K_{RF}(t)$ in eq. (4) is not a step function but simply sinusoidal. We, however, superimposed another weak sinusoidal driving force to simulate a breakdown of lattice symmetry [13]. The three curves in Fig. 5 were obtained with different ratios of the perturbation wave amplitude to the primary focusing wave amplitude. The additional perturbation wave reduces the lattice superperiodicity from twelve (N_{sp} = 12) to three (N_{sp} = 3), which has caused sharp drops of confinable ion number near the bare tunes $\nu_0 \approx 3n/2m$. The slight shifts from this condition are attributed to the term $C_m\Delta\nu$ in eq. (6). The two neighboring stop bands slightly above ν_0 = 3/4 and 3/2 are due to the linear and nonlinear resonances. The narrow stronger resonance on the left side should be the m = 2 instability (linear) while unstable nonlinear modes are responsible for the broader band on the right. The separation of the linear and nonlinear stop bands can be explained by the difference of C_m's. In fact, C_m is slightly larger for a higher-order mode [10,12]. Each curve in Fig. 5 contains several hundred independent measurement results, but the whole experimental procedure was automatically completed within a few hours.

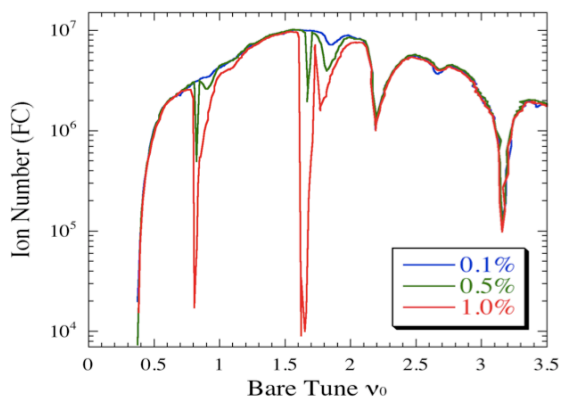

Figure 5: Number of Ar^+ ions that survived after 1 msec storage in a LPT [5].

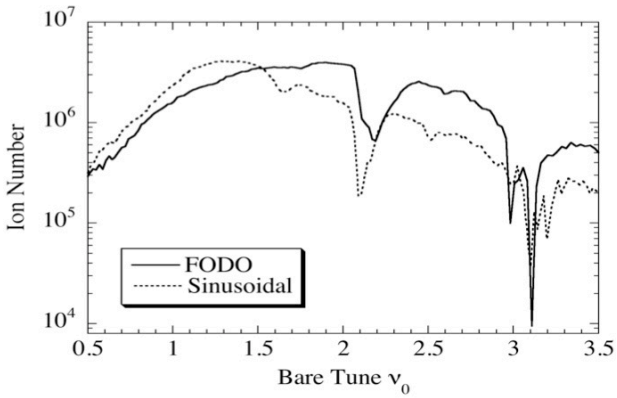

Figure 6: Resonance stop bands of sinusoidal and pulsed (FODO) focusing.

We have also measured the stop band distributions when a FODO waveform, instead of the sinusoidal excitation, is employed for ion confinement. A result is given and compared with the corresponding sinusoidal case in Fig. 6. The filling factor of FODO is set at 50% in this example. The figure suggests that the resonance condition remains almost unchanged even if the RF waveform is switched to the FODO type. This observation is consistent to the theoretical predictions based on the 2D Vlasov-Poisson equations [11]. We have also confirmed that 2D numerical simulations with the PIC code "WARP" [14] support the experimental result.

Resonance Crossing

When a beam is strongly cooled in a storage ring, a large space-charge-induced tune shift may make the effective operating point of the machine reach or even go across a resonance stop band [15]. Resonance crossing is also a major issue in non-scaling type FFAG accelerators where the bare tune inevitably varies over a wide range in the process of RF acceleration [16]. The S-PODs allow us to investigate these important issues systematically. Since the Doppler cooling system is equipped, an arbitrary amount of tune shift can be made in practice. The cooling efficiency is controllable with the laser power and the speed of laser-frequency scanning.

For the study of resonance crossing in FFAG, we simply reduce the amplitude of the RF quadrupole field from a certain value (corresponding to the initial bare tune of the machine) to another (corresponding to the final tune at beam extraction) at a certain speed (corresponding to the actual acceleration efficiency by RF cavities). As demonstrated in Fig. 5, it is an easy matter in S-POD to create non-intrinsic stop bands due to lattice asymmetry and/or error fields. A new LPT is now being prepared for this novel resonance-crossing experiment.

HALO EXPERIMENTS

Another SCE of practical importance that needs further careful investigations is the "halo formation". A systematic experimental study of halo formation mechanisms is clearly tough because of many reasons. For instance, the halo is only a small portion of the whole beam moving at high speed, so it is difficult to measure this low-density part at sufficiently high resolution. Besides, as mentioned above, we are not allowed to lose too many high-energy particles in real machines (while we are particularly interested in the halo formation from high-power beams). Note also that precise control of "mismatch (sudden disturbance to a stationary beam)" is required for the study of this collective effect. In any large complex machines, however, there exist many possible sources of mismatches that cause us trouble figuring out the correct parameter dependence of halo properties.

We have used the MRET to clarify the basic features of beam halos induced by external disturbance. The scaled Hamiltonian for electrons in the MRET can be written, in a proper rotating frame, as

$$H_{\mathrm{MRET}} = \frac{p_x^2 + p_y^2 + p_z^2}{2} + \frac{1}{2}\kappa_c^2 r^2 + I_2(\phi_{\mathrm{RE}} + \phi), \qquad (7)$$

where I_2 is a constant, κ_c is proportional to the cyclotron frequency, and $r^2 = x^2 + y^2$. The additional scalar potential ϕ_{RE} generated by the DC voltages on the ring electrodes is approximated to be

$$\phi_{\mathrm{RE}} = gV_0(z^2 - r^2/2), \qquad (8)$$

where g denotes the form factor determined by the trap geometry, and V_0 is the electrostatic potential depth for axial electron confinement. Similarities between the MRET Hamiltonian in eq. (7) and the smoothed system in eq. (5) are obvious.

In order to apply a mismatch to an electron plasma confined in the MRET, we quickly change either the axial magnetic field **B** or the electrostatic potential ϕ_{RE}. A fast switch of the **B** field is, however, not easy in the present system. We have thus produced a mismatch by increasing or decreasing the ring electrode potential V_0 as quickly as possible after a certain period of plasma storage (typically, 20 μsec). This procedure gives major longitudinal disturbance to the plasma. Although the radial motion is simultaneously disturbed according to eq. (8), the resultant transverse mismatch is weak because the magnetic field dominates the radial confinement [17]. Typical experimental parameters are listed in Table 1. A rather weak **B** field is chosen in order to lower the Brillouin density limit. We expect that the *local* tune depression reaches around 0.5. After the switch of V_0, we wait for a while and finally remove the potential wall on the detector (phosphor) side of the MRET to measure the

Table 1: Typical MRET Parameters for Halo Experiments

Confined particle	e^-
Axial magnetic field	62.5 Gauss
Electric potential depth	(40 – 60) V
Number of confined particles	~ 10^8
Cyclotron angular frequency	1.1 GHz

transverse profile of the plasma. Figure 7 is an example of the phosphor outputs with and without the mismatch. The axial potential depth was changed from 40 V to 60 V within 0.25 μsec in this case. Although the plasma experienced largely a longitudinal disturbance, we observe a clear halo developed in the radial direction. Since the plasma has an ellipsoidal shape (with an aspect ratio > 10), it is not straightforward to estimate the amount of halo particles from this transverse profile data, but we suspect that about 15% (or perhaps even more) of the whole plasma has contributed to this halo. We have also confirmed experimentally that the halo is weakened (and eventually disappears) as we decrease the magnitude of the potential jump.

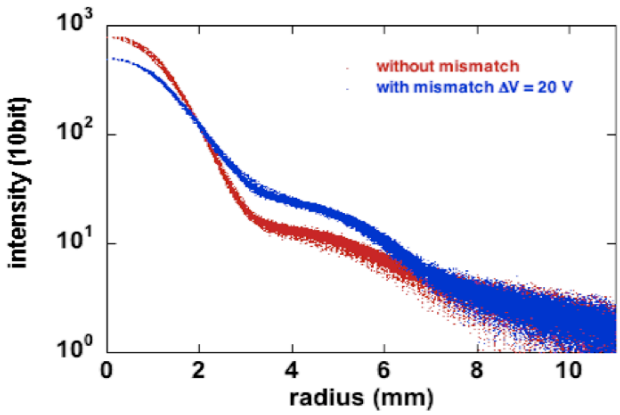

Figure 7: Transverse profiles of electron plasmas with and without a potential disturbance.

CONCLUDING REMARKS

The S-PODs, the compact non-neutral plasma trap systems at Hiroshima University, are already in full operation, accumulating useful information of collective effects in space-charge-dominated particle beams. Following the idea in ref. [2], both RF and magnetic traps were constructed, each of which has been applied to different beam physics purposes. So far, we have mostly concentrated upon resonance-related issues and mismatch-induced halo formation studies. Two S-PODs have been used for the former purposes [5] and ultralow-emittance ion source experiments [6]. In addition, we are now testing the third S-POD that will soon be employed for resonance crossing experiments and others. Another type of S-POD based on the MRET is also producing systematic experimental data on halo formation under various conditions. We plan to do similar halo experiments with ion plasmas in the multi-sectioned LPTs where the LIF diagnostics is available.

The present novel experimental technique offers a promising future option to deepen understanding of collective beam behaviors. The S-PODs have already demonstrated a high potential for advanced SCE studies, providing detailed data of resonance instabilities and halo formation. In order to further improve this technique, it should be valuable to carry out supporting numerical simulations that help us to interpret what we observe. It is also worthy to try developing more diagnostic options for precise plasma measurements.

ACKNOWLEDGEMENTS

Many students belonging to the Beam Physics Group of Hiroshima University have contributed to the development of the trap systems described here. The authors would also like to thank Dr. Steven M. Lund for valuable discussion and support in the course of this work. This experimental project was supported in part by a Grant-in-Aid for Scientific Research, Japan Society for the Promotion of Science, and by High Energy Accelerator Research Organization.

REFERENCES

[1] See, e.g., *Handbook of Accelerator Physics and Engineering*, edited by A. W. Chao and M. Tigner (World Scientific, Singapore, 1998).
[2] H. Okamoto and H. Tanaka, Nucl. Instrum. Meth. A **437**, 178 (1999).
[3] H. Okamoto, Hiroshima University Preprint HUBP-01/98 (1998).
[4] P. K. Ghosh, Ion Traps (Oxford Science, Oxford, 1995), and references therein.
[5] S. Ohtsubo, M. Fujioka, H. Higaki, K. Ito, H. Okamoto, H. Sugimoto, and S. M. Lund, Phys. Rev. STAB **13**, 044201 (2010).
[6] K. Izawa, K. Ito, H. Higaki, and H. Okamoto, J. Phys. Soc. Jpn. **79**, 124502 (2010).
[7] R. C. Davidson, H. Qin, and G. Shvets, Phys. Plasmas **7**, 1020 (2000).
[8] E. P. Gilson, R. C. Davidson, P. C. Efthimion, and R. Majeski, Phys. Rev. Lett. **92**, 155002 (2004).
[9] M. Chung *et al.*, Phys. Rev. Lett. **102**, 145003 (2009).
[10] F. J. Sacherer, Ph.D thesis, Lawrence Radiation Laboratory [Report No. UCRL-18454, 1968].
[11] I. Hofmann, L.J. Laslett, L. Smith, and I. Haber, Part. Accel. **13**, 145 (1983).
[12] H. Okamoto and K. Yokoya, Nucl. Instrum. Meth. A **482**, 51 (2002).
[13] Since $K(t)$ is a periodic function in a circular machine, we can expand it into a Fourier series. The amplitude of each harmonics depends on the lattice design and random gradient errors. Among many Fourier components, only two most dominant harmonics have been considered in this experiment. For more detailed information of the experimental conditions, see ref. [5].
[14] D. P. Grote, A Friedman, G. C. Craig, I. Haber, and W. M. Sharp, Nucl. Instrum. Meth. A **464**, 563 (2001).
[15] K. Okabe and H. Okamoto, Jpn. J. Appl. Phys. **42**, 4584 (2003).
[16] C. Johnstone et al., Proc. PAC'99 (New York, March 1999) p.3068.
[17] The transverse mismatch is well below 10% but may have non-negligible effect on halo formation.